Bulletin of the Seismological Society of America, Vol. 92, No. 4, pp. 1525–1542, May 2002

TriNet Strong-Motion Data from the *M* 7.1 Hector Mine, California, Earthquake of 16 October 1999

by Vladimir Graizer, Anthony Shakal, Craig Scrivner, Egill Hauksson, Jasha Polet, and Lucy Jones

Abstract The M_w 7.1 Hector Mine earthquake of October 16, 1999 was recorded by more than 300 stations of TriNet, which is administered cooperatively by the California Division of Mines and Geology's California Strong Motion Instrumentation Program (CDMG/CSMIP), California Institute of Technology, and the U.S. Geological Survey (USGS). The earthquake occurred in a remote part of the Mojave Desert, approximately 190 km northeast of downtown Los Angeles, and there were no strong-motion stations close to the surface rupture. The nearest station, Hector, is about 27 km north of the epicenter; it recorded a peak horizontal ground acceleration of 0.33*g*. The two next closest stations, Amboy and Joshua Tree, are to the east and south, both at epicentral distances of about 50 km; each recorded peak ground accelerations of about 0.2*g*. The new digital instruments installed for the TriNet project recorded a large set of reliable data at epicentral distances up to 275 km. These data can significantly improve empirical peak ground motion attenuation relationships, which are usually developed for distances only up to 100 km (Boore *et al.*, 1993, 1997) because adequate data have not been available at greater distances.

Hector Mine peak ground motions demonstrate reasonable agreement with empirical attenuation relationships for acceleration. In contrast, higher than expected ground velocities and displacements were recorded at epicentral distances of about 150 to 220 km, especially in the Los Angeles sedimentary basin, where anomalously high-amplitude displacements with periods of 6 to 7 sec were recorded in Los Angeles, Long Beach, and other areas. These long-period surface- or basin-generated waves can have significant effects on large structures.

The M_w 7.3 Landers earthquake of 1992 similarly produced strong, long-period waves in the basin. The peak ground motions produced by the Landers earthquake were on average 1.6 times higher than for the Hector Mine earthquake in the Los Angeles area.

Ground-motion data recorded by digital instruments were uniformly processed in the frequency band 0.067 to 46 Hz (0.022–15 sec). The processed data set includes records from 213 ground-response stations. In an effort to make strong-motion data available quickly to the engineering and scientific communities, important records from this event were made available by file transfer protocol (ftp) beginning the day of the earthquake.

Introduction

The M_w 7.1 Hector Mine, California, earthquake occurred on 16 October 1999 at 2:46 a.m. PDT in a remote part of the Mojave Desert area, approximately 190 km northeast of downtown Los Angeles. The hypocenter is located at 34.59°N and 116.27°W at a depth of 5 km (Hauksson *et al.*, 2002). The earthquake produced approximately 45 km of surface faulting along part of the Bullion fault and the previously unnamed Lavic Lake fault, as well as parts of several other faults (Treiman *et al.*, 2002). The fault mechanism was right-lateral strike slip, with an observed average slip of 250 to 300 cm across the entire fault zone and vertical displacements of 100 cm or less (Trelman *et al.*, 2002). The rupture was located approximately 20 to 30 km east-northeast of the 1992 M_w 7.3 Landers fault rupture.

The Hector Mine earthquake was recorded by more than 300 strong-motion stations of TriNet, which is administered

by the California Strong Motion Instrumentation Program (Division of Mines and Geology), California Institute of Technology, and the U.S. Geological Survey (Mori *et al.*, 1999). The station HEC near Hector was the closest seismic station, located approximately 27 km north of the epicenter (10.7 km from the nearest part of the rupture); it recorded a peak horizontal ground acceleration of 0.33*g*. The two other stations closest to the epicenter were Amboy and Joshua Tree. They are located to the east and south, at epicentral distances of about 50 km, and recorded peak ground accelerations of 0.18 and 0.19*g*, respectively. Maximum values of ground acceleration, velocity, and displacement recorded by the TriNet ground-response stations are listed in Table 1. To make comparison of processed data easier, all digital records were processed uniformly in the same frequency band: 0.067 to 46 Hz (0.022–15 sec). The data set includes records from 213 ground-response stations.

In contrast to the strong-motion data sets recorded largely by analog instruments during the 1992 Landers and the 1994 Northridge earthquakes (e.g., Shakal *et al.*, 1992, 1994; Cramer and Darragh, 1994), most of the data recorded during the Hector Mine earthquake were obtained using digital instruments. The second main difference is that no large-amplitude, near-source ground motions were recorded during the Hector Mine event, because of the sparse distribution of stations in the Mojave Desert area. The new digital instrumentation installed in the TriNet project recorded a large set of reliable data at epicentral distances up to 275 km. The recorded strong-motion data can be used in earthquake source- and wave-propagation modeling and in engineering analysis of ground shaking. These data can also be used to significantly improve empirical peak horizontal ground motion attenuation relationships, which are usually developed for distances of only 100 km or less (Boore *et al.*, 1993, 1997) because not enough reliable data have been available for greater distances.

Highlights of Ground-Response Strong-Motion Records

A list of all processed records from the TriNet ground-response stations used in this article is given in Table 1. The stations are listed in order of increasing epicentral distance. The processed time series for acceleration, velocity, and displacement at six ground-response stations were selected to highlight important features of the data set. The records from Big Bear Lake–Fire Station (epicentral distance $r = 68$ km), Wrightwood–Nielson Ranch ($r = 121$ km), Altadena–Eaton Canyon Park ($r = 174$ km), Downey–County Maintenance Bldg. ($r = 190$ km), Long Beach–Los Coyotes and Stearns ($r = 193$ km), and Los Angeles–116th Street School ($r = 197$ km) are shown in Figure 1. For all records, 80-sec time intervals are shown.

Peak ground acceleration generally decreases with increasing epicentral distance at the selected stations (Table 2), but the table also shows that peak ground velocities (PGV) and peak ground displacements (PGD) do not follow a simple attenuation pattern.

Displacement waveforms at the first three stations are similar in shape, and are characterized by approximately 15 to 20 sec of relatively simple motion (Fig. 1). This motion may be associated with the *S* wave coming from the earthquake source, with a period of approximately 6 to 8 sec. The maximum amplitude of this displacement generally decreases with increasing epicentral distance to about 100 km, beyond which it remains nearly constant at about 4 cm. This simple type of ground displacement also can be seen at many stations at epicentral distances up to 240 km (e.g., Pacoima, Sylmar, Newhall, Tarzana, and Moorpark; see Table 1). According to Dreger and Kaverina (2000a,b), the major part of the seismic moment was released within 20 sec during the Hector Mine earthquake. This time interval corresponds to the duration of the recorded *S*-wave motion.

The long-period part of the velocity and displacement waveforms are significantly amplified in the Long Beach and Los Angeles areas, with displacements up to 15 cm and corresponding maximum horizontal velocities up to 13 cm/sec. Those are approximately the same levels as at the closest stations. Ground motions with long-duration wavetrains after the *S*-wave arrival were recorded at a large number of stations. Long duration (40–60 sec) and high amplitudes of long-period (6–8 sec) waves may be due to the basin waves or surface waves generated in the basin. These waves have approximately the same periods as the source-generated *S* waves.

Response spectra (5% damped; Fig. 2a) of the N–S components of acceleration calculated for the three closest stations (Big Bear, Wrightwood, and Altadena; Fig. 1a–c) have maximum amplitudes at periods around 0.2 to 0.7 sec (frequencies 1.4–5.0 Hz), with much lower amplitudes at longer periods. In contrast to those three stations, spectral accelerations at the stations in the Los Angeles basin (Downey, Long Beach, and Los Angeles; Fig. 2b) contain a very strong long-period (5–8 sec) component. This motion can also be seen in the time domain (Fig. 1d–f).

Some stations in other areas also demonstrate relatively long duration of long-period motion. For example, the two stations on deep sediments in the San Bernardino area (San Bernardino–E and Hospitality, $r = 111$ km, and San Bernardino–Mountain. View and Cluster, $r = 108$ km) demonstrate up to 40 sec of long-period (5–6 sec), high-amplitude motions. Ground motions at other stations over shallow sediments in the San Bernardino area (San Bernardino–Highland and Del Rosa, $r = 104$ km; Highland, $r = 102$ km; and Rialto, $r = 117$ km) are more similar in shape to the motion at the Big Bear, Wrightwood, and Altadena stations, with the duration of main motion up to 20 sec and much lower amplitudes (see Table 1). These large variations in strong motion may be due to the differences in wave propagation path and site geology, especially the varying thickness and depth of the relatively soft sedimentary basin layers. Records in Salton City (148 km) and El Centro

Table 1
Peak Horizontal Ground Motions at TriNet Stations during the Hector Mine Earthquake

Station ID	Station Name	Network	Lat	Long	Epi Dist (km)	Fault Dist (km)	Accel (g)	Vel (cm/sec)	Displ (cm)
HEC	Hector	SCSN	34.83	116.33	27.2	10.7	0.330	44.5	13.4
21081	Amboy	CDMG	34.56	115.74	48.5	45.8	0.180	27.3	14.0
22170	Joshua Tree–Fire Station	CDMG	34.13	116.31	51.2	22.6	0.190	23.2	6.5
22791	Big Bear Lake–Fire Station	CDMG	34.24	116.87	67.5	65.3	0.170	13.3	9.2
22161	Twentynine Palms–Joshua Tree N.M.	CDMG	34.02	116.01	67.5	40.1	0.060	6.6	5.3
22T04	Heart Bar State Park	CDMG	34.16	116.80	68.1	60.9	0.082	11.6	8.3
12149	Desert Hot Springs–Fire Station	CDMG	33.96	116.51	73.1	47.1	0.082	7.5	3.8
12647	Joshua Tree N.M.–Keys View	CDMG	33.92	116.17	74.3	47.7	0.089	7.9	4.8
32075	Baker–Fire Station	CDMG	35.27	116.07	77.8	54.7	0.130	10.1	3.1
23559	Barstow–Vineyard & H St.	CDMG	34.89	117.05	78.4	57.9	0.070	7.8	3.9
DAN	Danby	SCSN	34.64	115.38	81.7	77.0	0.130	10.3	6.6
32577	Fort Irwin	CDMG	35.27	116.68	84.2	59.9	0.130	14.3	7.9
12630	Snow Creek	CDMG	33.89	116.68	86.7	65.2	0.029	3.8	3.1
12674	Banning–Twin Pines Rd.	CDMG	33.87	116.82	94.9	77.7	0.021	4.0	4.0
12543	Indio–Riverside Co. Fairgrounds	CDMG	33.72	116.22	97.2	71.1	0.120	19.0	13.6
12026	Indio–Coachella Canal	CDMG	33.72	116.15	97.4	70.8	0.124	13.7	7.7
12919	Beaumont–6th & Maple	CDMG	33.93	116.97	97.7	87.3	0.062	13.4	10.7
23583	Hesperia–4th & Palm	CDMG	34.40	117.31	98.0	90.6	0.063	10.1	5.5
HLN	Highland	SCSN	34.12	117.22	101.6	96.0	0.036	8.8	6.4
23897	San Bernardino–Highland & Del Rosa	CDMG	34.13	117.25	103.6	102.6	0.045	8.3	7.5
12618	San Jacinto–Soboba A	CDMG	33.80	116.88	103.9	85.5	0.061	6.9	3.9
12624	Lake Cahuilia–County Park	CDMG	33.63	116.28	106.7	81.2	0.025	4.0	2.0
23732	San Bernardino–Devil Canyon Penstock	CDMG	34.19	117.33	107.1	104.8	0.023	7.4	6.1
23780	San Bernardino–Mtn. View & Cluster	CDMG	34.10	117.29	108.3	105.3	0.061	18.3	9.3
23898	San Bernardino–Medical Cntr & Highland	CDMG	34.13	117.32	109.1	108.1	0.060	10.1	9.4
12673	San Jacinto–CDF Fire Station	CDMG	33.79	116.96	109.3	92.9	0.060	18.2	16.0
23542	San Bernardino–E & Hospitality	CDMG	34.06	117.29	110.6	107.8	0.072	16.0	10.9
13927	Moreno Valley–Alessandro & Moreno Bch	CDMG	33.92	117.17	111.5	103.8	0.062	5.7	5.9
12923	Hernet–Acacia & Stanford	CDMG	33.74	116.93	111.9	92.9	0.063	13.3	5.8
13926	Moreno Valley–Hwy 60 & Heacock	CDMG	33.94	117.25	115.4	109.1	0.050	6.0	5.4
23597	Phelan–Wilson Ranch Road	CDMG	34.47	117.52	115.6	105.5	0.073	7.5	3.7
12331	Hemet–Stetson Ave Fire Station	CDMG	33.73	116.98	115.7	97.6	0.067	6.8	3.7
11825	Mecca–CVWD Yard	CDMG	33.56	115.99	116.8	89.5	0.100	19.9	14.8
23899	Rialto–I10 & Cedar	CDMG	34.07	117.40	118.8	117.0	0.036	5.2	4.9
13915	Riverside–I215 & 3rd	CDMG	33.98	117.34	119.9	115.5	0.054	6.4	4.5
23912	Fontana–Arrow & Sierra	CDMG	34.10	117.43	120.1	118.5	0.046	6.0	5.3
FON	Fontana	SCSN	34.10	117.44	120.5	118.8	0.040	6.4	5.3
23573	Wrightwood–Nielson Ranch	CDMG	34.31	117.54	121.1	114.2	0.054	5.0	4.4
13924	Homeland–Hwy 74 & Sultanas	CDMG	33.75	117.13	122.3	110.7	0.040	3.2	3.9
13916	Riverside–Van Buren & Trautwein	CDMG	33.90	117.32	123.7	117.2	0.034	4.1	4.2
13928	Perris–San Jacinto & C St.	CDMG	33.79	117.23	125.6	115.9	0.018	4.0	3.8
13930	Sun City–I215 & McCall Blvd	CDMG	33.72	117.19	128.8	117.4	0.041	3.9	3.5
13123	Riverside–Airport	CDMG	33.95	117.45	129.4	125.4	0.025	4.1	4.0
12626	Desert Shores	CDMG	33.43	116.08	130.3	103.4	0.039	3.0	2.0
13921	Riverside–Limonite & Downey	CDMG	33.97	117.49	131.1	127.9	0.029	4.6	4.4
23585	Palmdale–Black Butte	CDMG	34.59	117.73	133.8	120.7	0.019	2.8	1.8
13913	Riverside–Hole & La Sierra	CDMG	33.92	117.49	134.6	130.3	0.036	4.3	3.9
13929	Menifee Valley–Murrieta & Scott	CDMG	33.65	117.21	135.4	123.2	0.032	3.1	3.6
11591	North Shore–Durmid	CDMG	33.42	115.83	135.9	108.4	0.075	15.1	10.4
23896	Ontario–I10 & 4th	CDMG	34.08	117.62	136.7	133.8	0.031	7.2	5.4
23590	Wrightwood–Jackson Flat	CDMG	34.38	117.74	136.7	127.5	0.045	6.4	3.7
11627	Bombay Beach–Bertram	CDMG	33.40	115.78	140.0	112.5	0.035	11.2	10.4
23895	Ontario–4th & Mountain	CDMG	34.08	117.67	140.9	137.6	0.034	8.2	7.5
13918	Norco–1st & Hamner	CDMG	33.90	117.56	141.2	137.2	0.016	4.3	4.0
13922	Lake Elsinore–Graham & Poe	CDMG	33.67	117.33	141.5	131.1	0.034	5.4	5.4
13726	Corona–Calif. Ave.	CDMG	33.85	117.54	142.6	137.5	0.031	4.8	4.1
CRN	Corona	SCSN	33.88	117.56	143.0	138.4	0.030	5.0	4.2
11684	Frink	CDMG	33.40	115.66	143.8	116.5	0.072	11.7	5.4
13172	Temecula–CDF	CDMG	33.50	117.15	146.0	123.5	0.057	9.0	3.9
11628	Salton City	CDMG	33.28	115.98	147.7	120.6	0.055	7.1	4.4

(*continued*)

Table 1
Continued

Station ID	Station Name	Network	Lat	Long	Epi Dist (km)	Fault Dist (km)	Accel (g)	Vel (cm/sec)	Displ (cm)
23525	Pomona–4th & Locust	CDMG	34.06	117.75	148.4	144.8	0.037	8.4	6.3
23837	Pomona–Orange Grove & Fairplex	CDMG	34.06	117.78	151.1	147.1	0.034	6.9	5.9
23836	Glendora–Gladstone & Sunflower	CDMG	34.11	117.85	154.7	149.2	0.038	6.6	6.0
13122	Featherly Park–Maint. Bldg.	CDMG	33.87	117.71	154.8	151.4	0.041	6.9	6.7
23595	Littlerock–Brainard Canyon	CDMG	34.49	117.98	157.4	145.6	0.034	3.6	2.7
LTR	Littlerock	SCSN	34.52	117.99	158.1	145.7	0.054	4.3	2.4
13882	Olinda–Carbon Canyon Rd	CDMG	33.93	117.80	159.2	157.1	0.042	8.4	7.4
23774	West Covina–Kaiser Grounds	CDMG	34.07	117.94	164.0	158.8	0.027	11.1	12.1
13849	Anaheim–Lakeview & Riverdale	CDMG	33.85	117.82	164.3	161.3	0.056	13.1	10.5
23843	La Puente–Amar & Hacienda	CDMG	34.04	117.95	166.4	161.7	0.040	13.7	10.6
13873	Brea–Central Av Caltrans Yard	CDMG	33.93	117.90	166.6	163.7	0.026	10.5	8.3
23842	City of Industry–Gale & Azusa	CDMG	34.00	117.93	166.6	162.6	0.048	9.8	7.3
13883	Anaheim–Kraemer & La Palma	CDMG	33.85	117.86	167.5	164.8	0.040	12.4	11.0
23773	Baldwin Park–Kaiser Grounds	CDMG	34.07	117.98	168.0	162.7	0.025	14.4	12.8
13878	Fullerton–CSU Fullerton Grounds	CDMG	33.89	117.89	168.0	165.8	0.042	12.2	11.2
13888	Orange–Shaffer & Taft	CDMG	33.82	117.85	168.8	165.5	0.029	9.9	10.3
13875	Orange–Hwy 22/Hwy 55 Grounds	CDMG	33.78	117.83	169.9	165.8	0.036	10.4	6.4
OGC	Orange	SCSN	33.79	117.84	170.2	166.3	0.045	9.8	7.4
13880	Fullerton–Hermosa & Harbor	CDMG	33.91	117.93	170.5	167.8	0.030	11.8	11.0
13881	La Habra–La Habra & Monte Vista	CDMG	33.93	117.96	171.5	168.3	0.036	11.7	8.7
FUL	Fullerton	SCSN	33.87	117.92	171.8	169.7	0.040	17.1	17.6
24850	Whittler–Workman Mill Rd & Pomona Fwy	CDMG	34.03	118.02	172.5	167.5	0.038	11.0	8.9
13889	Santa Ana–I5 & 4th St	CDMG	33.75	117.84	172.6	168.1	0.029	8.7	7.6
24402	Altadena–Eaton Canyon Park	CDMG	34.18	118.10	174.1	166.6	0.037	4.9	4.0
13893	Orange–I5 & Chapman	CDMG	33.78	117.89	174.1	170.4	0.039	13.6	9.2
14840	Whittler–Scott & Whittler	CDMG	33.95	118.00	174.6	170.9	0.042	11.5	10.2
13879	Fullerton–Valencia & Brookhurst	CDMG	33.87	117.96	175.0	172.7	0.046	16.7	12.0
KIK	Pasadena–Kinemetrics	SCSN	34.15	118.10	175.4	168.2	0.023	5.7	4.0
13894	Garden Grove–Chapman & West	CDMG	33.79	117.92	176.3	173.0	0.043	12.8	11.3
13890	Santa Ana–1st & Franklin	CDMG	33.74	117.89	176.8	172.6	0.038	13.1	10.0
24576	Anaverde Valley–City Ranch	CDMG	34.58	118.20	177.0	163.5	0.038	3.7	1.6
13884	Garden Grove–Hwy 22 & Harbor Blvd	CDMG	33.77	117.92	177.3	173.6	0.035	12.4	11.1
13892	Santa Ana–Macarthur & Bristol	CDMG	33.70	117.88	178.3	173.3	0.039	7.9	6.9
SJU	San Juan Capistrano	SCSN	33.49	117.68	178.7	169.2	0.026	8.1	6.8
24841	Pico Rivera–Durfee & Whittler	CDMG	34.00	118.08	178.7	173.8	0.021	8.5	7.2
24401	San Marino–SW Academy	CDMG	34.12	118.13	179.1	172.3	0.018	3.6	3.6
13891	Santa Ana–Warner & Greenville	CDMG	33.72	117.90	179.2	174.6	0.050	10.6	7.9
13795	Capistrano Beach–I5/Via Calif. Bridge	CDMG	33.47	117.67	179.4	169.4	0.032	11.1	7.6
24691	Pasadena–Fair Oaks & Walnut	CDMG	34.15	118.15	179.7	172.4	0.040	4.9	3.2
13886	Garden Grove–Chapman & Gilbert	CDMG	33.79	117.97	179.9	176.9	0.034	15.0	12.6
24692	Pasadena–Orange Grove & Pasadena	CDMG	34.15	118.16	180.2	172.9	0.040	5.3	3.3
13885	Garden Grove–Brookhurst & Westminster	CDMG	33.76	117.96	180.8	177.2	0.032	11.9	12.8
24461	Alhambra–Fremont School	CDMG	34.07	118.15	182.4	176.2	0.024	5.7	5.5
13333	Oceanside B–Fire Station	CDMG	33.20	117.33	182.7	153.6	0.014	3.3	2.5
14828	Downey–Florence & I605	CDMG	33.94	118.10	183.2	179.0	0.041	10.0	8.8
24468	Los Angeles–CSULA Admin. Building	CDMG	34.07	118.17	184.1	177.8	0.040	10.0	8.9
13160	Newport Beach–Irvine Ave Fire Sta	CDMG	33.63	117.90	184.2	178.4	0.030	9.1	8.0
24592	Los Angeles–City Terrace	CDMG	34.05	118.17	184.8	178.7	0.038	6.7	5.3
13877	Newport Beach–Balboa Island	CDMG	33.60	117.89	185.1	178.8	0.034	6.5	5.5
24814	Los Angeles–Colorado & Eagle Rock	CDMG	34.14	118.21	185.3	177.9	0.025	3.0	3.1
LEV	Leona Valley	SCSN	34.61	118.29	185.4	171.4	0.050	3.8	2.0
24400	Los Angeles–Obregon Park	CDMG	34.04	118.18	186.0	180.1	0.033	6.6	6.3
14844	Bell Gardens–Garfield & Florence	CDMG	33.97	118.15	186.2	181.4	0.027	12.3	10.4
13887	Huntington Beach–Adams & Bushard	CDMG	33.68	117.96	186.2	181.4	0.052	9.8	9.4
14827	Downey–Imperial & Bellflower	CDMG	33.92	118.13	186.4	182.3	0.026	10.5	10.6
13876	Newport Beach–Balboa & Medina	CDMG	33.60	117.90	186.4	180.2	0.026	6.5	5.1
14874	Westminster–I405/Hwy 22 Grounds	CDMG	33.77	118.04	186.8	183.9	0.034	13.5	12.0
24605	Los Angeles–7-story Univ. Hospital Grnds	CDMG	34.06	118.20	186.9	180.5	0.020	5.4	4.8
14829	Bellflower–Flora Vista & Woodruff	CDMG	33.88	118.12	187.4	183.8	0.032	11.1	12.4
14830	Lakewood–Del Amo & Palo Verde	CDMG	33.85	118.11	118.2	185.2	0.044	13.5	14.7

(*continued*)

Table 1
Continued

Station ID	Station Name	Network	Lat	Long	Epi Dist (km)	Fault Dist (km)	Accel (g)	Vel (cm/sec)	Displ (cm)
24813	Cypress Park–San Fernando & Division	CDMG	34.10	118.23	188.5	181.6	0.025	3.5	3.0
14368	Downey–County Malnt. Bldg.	CDMG	33.92	118.17	189.7	185.3	0.033	13.3	10.9
13197	Huntington Beach–Lake St Fire Station	CDMG	33.66	118.00	189.7	185.0	0.031	9.0	7.9
14869	Long Beach–Los Coyotes & Palo Verde	CDMG	33.82	118.11	189.7	187.1	0.027	11.5	11.9
14825	Huntington Park–Saturn & Hood	CDMG	33.98	118.21	191.0	185.8	0.030	12.7	9.9
24812	Los Angeles–Rowena & Glendale	CDMG	34.11	118.26	191.0	183.8	0.020	3.2	2.3
24611	Los Angeles–Temple & Hope	CDMG	34.06	118.25	191.2	184.6	0.026	4.8	4.5
24839	Los Angeles–1st & Figueroa	CDMG	34.06	118.25	191.7	185.2	0.024	5.3	4.2
14872	Long Beach–Artesia & Orange	CDMG	33.87	118.18	192.7	188.9	0.031	12.8	10.9
14870	Long Beach–Los Coyotes & Steams	CDMG	33.80	118.14	193.1	190.5	0.031	12.4	11.7
24838	Los Angeles–Olive & Plco	CDMG	34.04	118.26	193.4	187.1	0.022	6.7	5.4
24752	Los Angeles–Griffith Park/Toyon(Rock)	CDMG	34.14	118.30	193.6	185.7	0.013	2.8	2.4
24612	Los Angeles–Pico & Sentous	CDMG	34.04	118.27	193.9	187.5	0.018	4.9	5.6
24853	Los Angeles–Beverly Blvd LADOT	CDMG	34.08	118.29	194.1	187.1	0.025	4.6	3.9
14826	Los Angeles–52nd & Central	CDMG	34.00	118.25	194.3	188.5	0.025	8.1	7.1
24976	Los Angeles–I10/110 Interchange Grnds	CDMG	34.04	118.28	194.4	188.1	0.020	5.2	5.5
14868	Long Beach–Willow & Cherry	CDMG	33.81	118.16	195.0	192.1	0.020	9.0	10.6
24816	Los Angeles–Vermont & Pico	CDMG	34.05	118.29	195.4	188.8	0.019	4.9	6.0
14823	Los Angeles–103rd & Compton	CDMG	33.94	118.25	195.6	190.5	0.032	10.5	8.9
24811	Los Angeles–Melrose & Western	CDMG	34.08	118.31	195.7	188.6	0.030	5.2	3.9
24852	Los Angeles–USC Fire Station	CDMG	34.02	118.28	195.7	189.5	0.015	6.5	5.5
24810	Hollywood–Franklin & Bronson	CDMG	34.10	118.32	195.9	188.5	0.035	4.5	3.3
14787	Los Angeles–MLK Hospital Grounds	CDMG	33.92	118.24	196.1	191.4	0.038	9.9	8.7
24709	Los Angeles–USC Grounds	CDMG	34.02	118.29	196.2	190.0	0.017	5.8	5.6
24088	Pacoima–Kagel Canyon Fire Sta	CDMG	34.30	118.38	196.2	186.1	0.032	5.5	4.7
14403	Los Angeles–116th St. School	CDMG	33.93	118.26	197.4	192.5	0.028	8.6	8.1
14871	Long Beach–Ocean Blvd & Cherry	CDMG	33.76	118.17	197.6	195.2	0.025	13.1	11.6
24271	Lake Hughes #1–Fire Station #78	CDMG	34.67	118.43	198.3	183.5	0.053	5.6	1.9
14847	Long Beach–Santa Fe Ave & I405	CDMG	33.83	118.22	198.3	194.9	0.023	11.9	10.7
14821	Los Angeles–Vermont & 78th	CDMG	33.97	118.29	198.4	192.8	0.030	7.6	8.1
24865	Universal City–Hwy 101 & Lankershim	CDMG	34.14	118.36	199.0	191.0	0.035	4.1	2.1
24809	Hollywood–Sunset & Fairfax	CDMG	34.10	118.35	199.2	191.8	0.019	3.6	3.1
14560	Long Beach–City Hall Grounds	CDMG	33.77	118.20	199.6	197.0	0.017	13.2	12.9
24851	Los Angeles–3rd & La Brea LADOT	CDMG	34.07	118.35	199.6	192.5	0.021	5.2	4.2
24815	North Hollywood–Laurel Cyn & Sherman	CDMG	34.20	118.40	200.3	191.4	0.029	5.4	4.6
24818	Los Angeles–Washington & La Brea	CDMG	34.04	118.35	200.7	194.0	0.017	5.1	5.1
14820	Los Angeles–54th & Crenshaw	CDMG	33.99	118.34	201.9	195.8	0.024	7.1	6.3
24763	Sylmar–Olive View Hospital Grounds	CDMG	34.33	118.44	201.9	191.3	0.030	5.9	4.4
14824	Los Angeles–Vermont & 182nd	CDMG	33.87	118.29	202.5	198.2	0.020	10.6	11.1
24765	Panorama City–Kaiser Hospital Grounds	CDMG	34.22	118.43	202.7	193.5	0.044	7.0	5.9
14537	Inglewood–Hollywood Park	CDMG	33.95	118.33	202.9	197.3	0.020	8.1	6.6
24808	Van Nuys–Burbank & Fulton	CDMG	34.17	118.42	203.1	194.5	0.028	5.9	4.2
24087	Arieta–Nordhoff Ave Fire Sta	CDMG	34.24	118.44	203.2	193.8	0.025	6.1	6.2
24801	Studio City–Ventura & Coldwater Cyn Av	CDMG	34.15	118.41	203.2	194.9	0.036	5.3	3.0
14834	Hawthome–Crenshaw & EI Segundo	CDMG	33.92	118.33	203.4	198.2	0.022	7.1	7.5
24703	Los Angeles–I10/La Cienega Geo. Array	CDMG	34.04	118.38	203.5	196.8	0.030	7.0	9.3
14846	Carson–Main & Sepulveda	CDMG	33.81	118.28	204.1	200.5	0.014	9.9	9.6
14835	Wilmington–Avalon & Anaheim	CDMG	33.78	118.26	204.3	201.2	0.017	9.7	9.8
24800	Mission Hills–Sepulveda & San Fernando	CDMG	34.27	118.46	204.7	194.7	0.028	7.9	7.3
24867	Van Nuys–Civic Center Grounds	CDMG	34.18	118.45	205.2	196.4	0.026	7.0	4.4
14767	Los Angeles–LAPD Manchester Cntr Grnds	CDMG	33.96	118.38	206.2	200.4	0.017	9.9	6.9
14785	Los Angeles–Vincent Thos. E Geo. Array	CDMG	33.75	118.27	206.6	203.8	0.024	12.3	10.0
14845	Harbor City–Normandle & Pac. Coast Hwy	CDMG	33.79	118.30	206.8	203.3	0.014	9.8	8.9
14822	Los Angeles–Century & Aviation	CDMG	33.94	118.38	207.1	201.4	0.017	7.4	7.4
14786	Los Angeles–Vincent Thos. W Geo. Array	CDMG	33.75	118.28	207.4	204.5	0.029	10.7	8.1
JFP	Jensen Filtration	SCSN	34.31	118.50	207.5	197.0	0.046	7.1	5.0
14831	Lomita–Narbonne & Pacific Coast Hwy	CDMG	33.79	118.32	208.6	205.0	0.015	9.1	8.3
24909	Los Angeles–I10/405 Freefield	CDMG	34.03	118.43	208.6	201.7	0.023	5.2	5.5
24819	Los Angeles–Veteran & Wilshire	CDMG	34.06	118.45	208.9	201.5	0.017	3.8	2.7
24279	Newhall–County Fire Sta.	CDMG	34.39	118.53	209.1	197.6	0.021	4.5	4.3

(*continued*)

Table 1
Continued

Station ID	Station Name	Network	Lat	Long	Epi Dist (km)	Fault Dist (km)	Accel (g)	Vel (cm/sec)	Displ (cm)
24586	Neenach–Sacatara Creek	CDMG	34.85	118.54	209.5	192.9	0.023	5.7	3.5
24802	Encino–Balboa & Ventura	CDMG	34.16	118.50	210.5	201.8	0.021	2.8	2.3
14159	San Pedro–Palos Verdes Fire Station	CDMG	33.72	118.31	211.2	208.5	0.008	4.0	3.2
24805	Northridge–Parthenia & Lindley	CDMG	34.23	118.53	211.3	201.7	0.039	10.5	6.9
24817	Los Angeles–Sunset & Kenter	CDMG	34.06	118.48	211.7	204.2	0.012	3.2	3.5
MIS	Mira Catallna School	SCSN	33.74	118.33	212.5	209.4	0.012	4.0	3.1
24T03	Tarzana–Clubhouse	CDMG	34.16	118.53	213.5	204.6	0.029	3.5	2.3
24764	Tarzana–Cedar Hill B	CDMG	34.16	118.53	213.6	204.8	0.055	5.1	2.1
24866	Reseda–Vanowen & Wilbur LADOT	CDMG	34.19	118.55	214.0	204.7	0.031	9.6	5.3
NOT	Northridge	SCSN	34.23	118.56	214.2	204.5	0.033	8.9	9.3
24806	Canoga Park–Winnetka & Roscoe	CDMG	34.22	118.57	215.4	205.7	0.032	9.7	6.4
1794	EI Centro–Meloland Geotechnical Array	CDMG	32.77	115.45	215.5	188.1	0.017	9.5	6.9
24278	Castaic–Old Ridge Route	CDMG	34.56	118.64	217.7	204.0	0.044	5.1	2.1
24277	Castaic–Hasley Canyon	CDMG	34.46	118.65	219.0	206.5	0.022	4.4	3.0
24807	Woodland Hills–Canoga & Ventura	CDMG	34.17	118.60	219.0	209.9	0.030	4.5	3.0
3748	San Diego–UCSD Hospital Grounds	CDMG	32.75	117.16	219.9	162.5	0.010	3.1	1.6
24804	West Hills–Roscoe & Fallbrook	CDMG	34.22	118.63	220.6	210.8	0.037	6.4	3.2
24803	Woodland Hills–Victory & Fallbrook	CDMG	34.19	118.62	221.0	211.7	0.028	5.6	3.6
24861	Simi Valley–Katherine Rd & Sylvan	CDMG	34.26	118.67	223.5	213.2	0.012	3.7	3.0
24644	Sandberg–Bald Mountain	CDMG	34.74	118.72	225.6	210.1	0.019	3.0	1.9
24860	Simi Valley–Church St & Los Angeles Av	CDMG	34.27	118.74	229.3	215.8	0.021	4.3	3.4
SMV	Simi Valley	SCSN	34.27	118.74	230.1	219.6	0.020	4.2	3.4
24855	Piru–Church St & Camulos	CDMG	34.41	118.80	232.8	220.6	0.031	6.6	3.4
24859	Oak Park–Kanan & Deerhill	CDMG	34.18	118.76	233.5	223.8	0.013	2.4	2.2
24396	Mallbu–Point Dume	CDMG	34.01	118.80	241.5	233.6	0.015	3.4	3.1
24283	Moorpark–Fire Station	CDMG	34.29	118.88	242.3	231.3	0.016	4.6	4.7
24864	Somis–Somis Rd	CDMG	34.26	119.00	253.2	242.3	0.016	3.6	2.7
24863	Camarillo–Woodcreek & Santa Rosa	CDMG	34.22	118.99	253.7	243.2	0.017	4.6	2.8
25282	Camarillo	CDMG	34.21	119.08	261.7	251.2	0.017	4.7	3.1
35365	Bakersfield–Stockdale & California	CDMG	35.35	119.05	268.0	248.0	0.008	2.9	3.6
25862	Oxnard–Hwy 101 & Oxnard Blvd	CDMG	34.24	119.18	270.2	259.2	0.014	7.8	6.6
25854	Ojai–Ojai Av & Fairway Ln	CDMG	34.45	119.23	272.2	259.3	0.013	2.7	1.9
44015	Lone Pine A	CDMG	36.60	118.06	275.9	251.1	0.015	4.3	3.5

(216 km) display an extremely-long duration (100–120 sec) of long-period (4–8 sec) motions. Surface waves generated in the deep sedimentary basins along the propagation path may be responsible for these effects.

In general, two types of ground displacement are observed during the Hector Mine earthquake:

1. One is a relatively simple motion with a duration of 15–20 sec. This type of motion can be observed everywhere, from 50 km up to 240 km from the epicenter. This motion may be associated with the source-generated *S* wave.
2. Motion of the second type is much longer in duration, about 40 sec; this type of motion is sinusoidal with a predominant period of about 5 to 8 sec. This type of motion is typical for certain locations in the Los Angeles, Long Beach, San Bernardino, and EI Centro areas. This displacement may be relatively high amplitude (more than 10 cm at the epicentral distances of about 200 km). The amplitude of this motion increases with time and reaches a maximum approximately 20 sec after the arrival of the *S* wave. This sinusoidal type of motion is most likely Love waves created by multiple reflections of *S* waves trapped in a deep sedimentary basin.

The N–S components of displacement waveforms recorded by 50 representative TriNet stations are shown on a map of southern California along with Quaternary, Tertiary, and Mesozoic (QTM) geology (Jennings, 1977; Park and Elrick, 1998) (Fig. 3). Surface fault rupture produced by the Hector Mine earthquake is shown in red in Figure 3 (Treiman *et al.*, 2002). The map shows the distribution of displacement waveforms relative to the fault and QTM geology (Jennings, 1994). Since the Hector Mine earthquake occurred in the Mojave Desert area, not many strong-motion stations that recorded the earthquake are located within 100 km of the epicenter. High-displacement amplitudes with long duration of ground motion occurred in the Los Angeles and Long Beach areas at the epicentral distance of about 200 km. Seismic waves with high amplitudes and long duration at periods of 5–8 sec may have significant effects on large structures.

In general, no direct correlation can be seen between

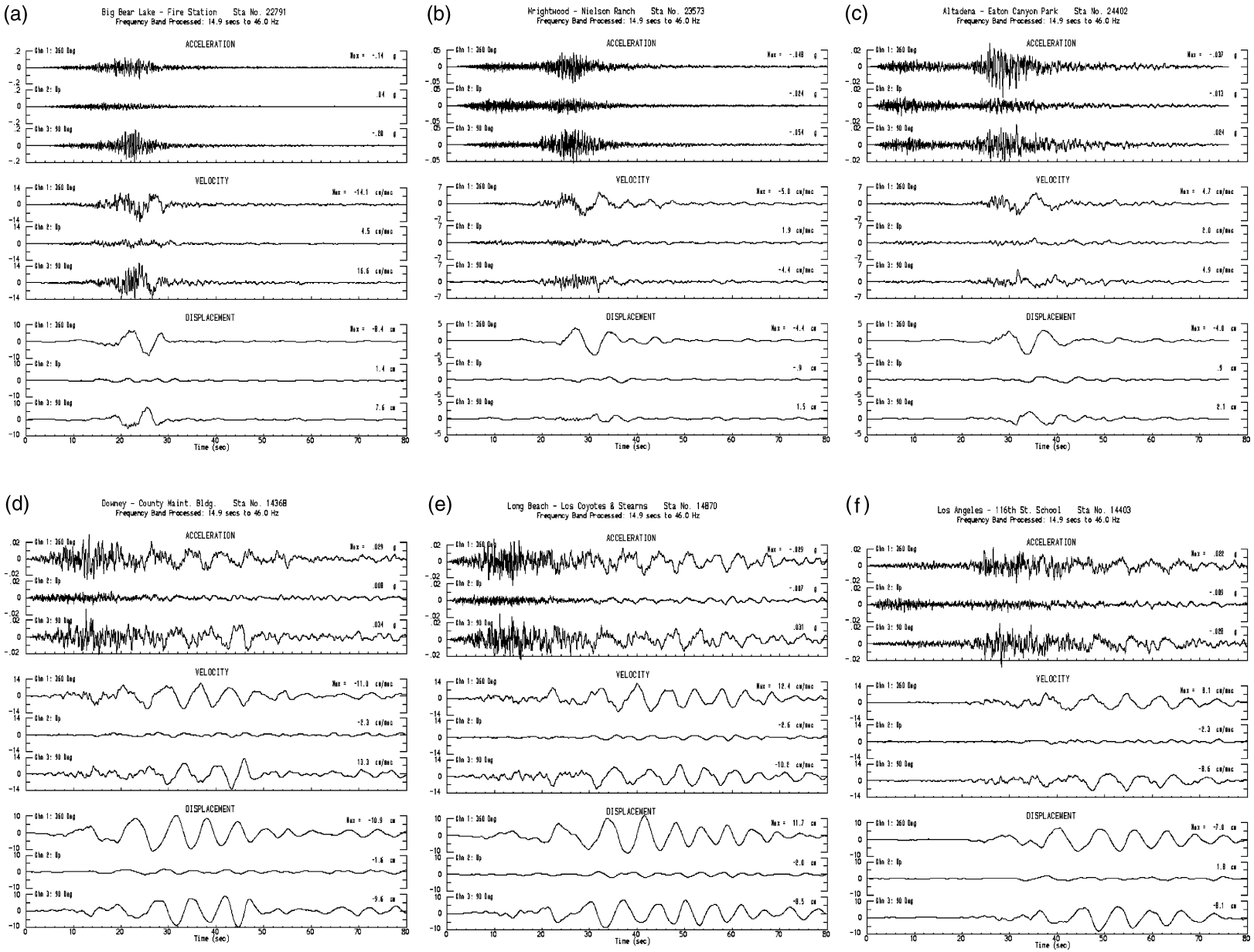

Figure 1. Acceleration, velocity, and displacement at six ground-response stations for the Hector Mine earthquake: (a) Big Bear Lake–Fire Station (epicentral distance $r = 68$ km), (b) Wrightwood–Nielson Ranch ($r = 121$ km), (c) Altadena–Eaton Canyon Park ($r = 174$ km), (d) Downey–County Maintenance Bldg. ($r = 190$ km), (e) Long Beach–Los Coyotes and Stearns ($r = 193$ km), and (f) Los Angeles–116th School ($r = 197$ km).

Table 2
Peak Horizontal Ground Motions for the Records Shown in Figure 1

Station ID	Station Name	Epi Dist (km)	PGA (*g*)	PGV (cm/sec)	PGD (cm)
22791	Big Bear Lake–Fire Station	68	0.20	16.6	8.4
23573	Wrightwood–Nielson Ranch	121	0.054	5.0	4.4
24402	Altadena–Eaton Canyon Park	174	0.037	4.9	4.0
14368	Downey–County Maintenance Bldg	190	0.034	13.3	10.9
14870	Long Beach–Los Coyotes & Stearns	193	0.031	12.4	11.7
14403	Los Angeles–116th St. School	197	0.028	8.6	8.1

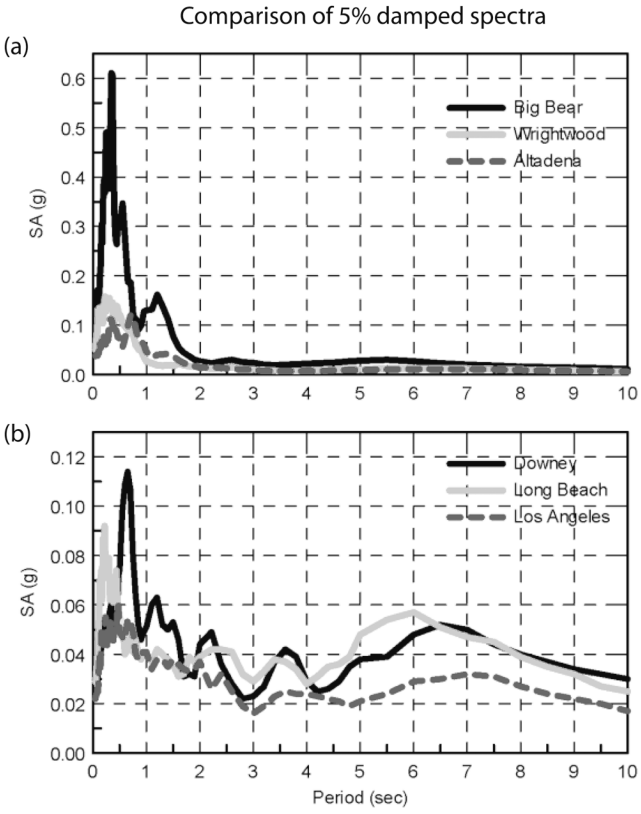

Figure 2. Response spectra (5% damped) of the N–S components for the six stations shown in Fig. 1: (a) for Big Bear, Wrightwood, and Altadena; (b) for Downey, Long Beach, and Los Angeles.

QTM geology and ground displacements. Figure 3 graphically shows large variations in displacements, as seen in some areas near the ocean, where both types of motion (the simple 15- to 20-sec long and the sinusoidal 40-sec long) were recorded at nearby stations. In this specific set of data, directivity does not appear to play a significant role; however, the spatial distribution of the strong-motion stations, located mostly to the west and south of the earthquake fault at epicentral distances of more than 80 km, is not favorable for studying directivity effects.

Response of Tarzana

Significantly amplified ground accelerations at the Tarzana station were recorded during the *M* 5.9 Whittier Narrows earthquake and during the *M* 6.7 Northridge earthquake and its aftershocks (Shakal *et al.*, 1988, 1996; Darragh *et al.*, 1997, 1998). In contrast, the Landers, Big Bear, and Sierra Madre mainshocks, and some other earthquakes, produced lower site amplifications. Amplified seismic response was observed at the Tarzana station during the Hector Mine earthquake (at an epicentral distance of 214 km), with peak horizontal ground acceleration almost twice as large as the accelerations recorded at other stations located at the same epicentral distance (Table 1).

The two strong-motion stations located at Tarzana–Cedar Hill B (having a three-component instrument at the surface and another one downhole at the depth of 60 m) and Clubhouse (about 180 m from Cedar Hill B, at the foot of Tarzana hill) have again demonstrated significant differences in maximum amplitudes of acceleration (0.055 and 0.036*g*, respectively) and velocity (5.0 and 3.5 cm/sec), with almost no difference in maximum displacements (2.5 and 2.4 cm). Figure 4 shows acceleration, velocity, and displacement time histories recorded at the downhole and two different surface locations. Ground motions were rotated to the directions parallel and perpendicular to the strike of the Tarzana hill.

Comparison of motions at the bottom and top of the hole shows significant amplification of accelerations (more than three times for the component perpendicular to the hill). In contrast to accelerations (high-frequency part of the seismic signal), displacements (relatively low-frequency part of the signal) demonstrate almost no site amplification from the bottom of the hole to the surface at long periods. Ground displacements at other CSMIP-instrumented downhole sites that recorded the Hector Mine earthquake also demonstrate almost no near-surface site amplification at longer periods (Graizer *et al.*, 2000a,b).

The downhole data are used as a reference to compare the amplification effect at the top of Tarzana hill (Hill B) and at the foothill (Clubhouse). Amplification from the bottom of the hole to the surface is similar along the component parallel to the strike of Tarzana hill to that at the foothill station, but the amplification from the bottom of the hole to

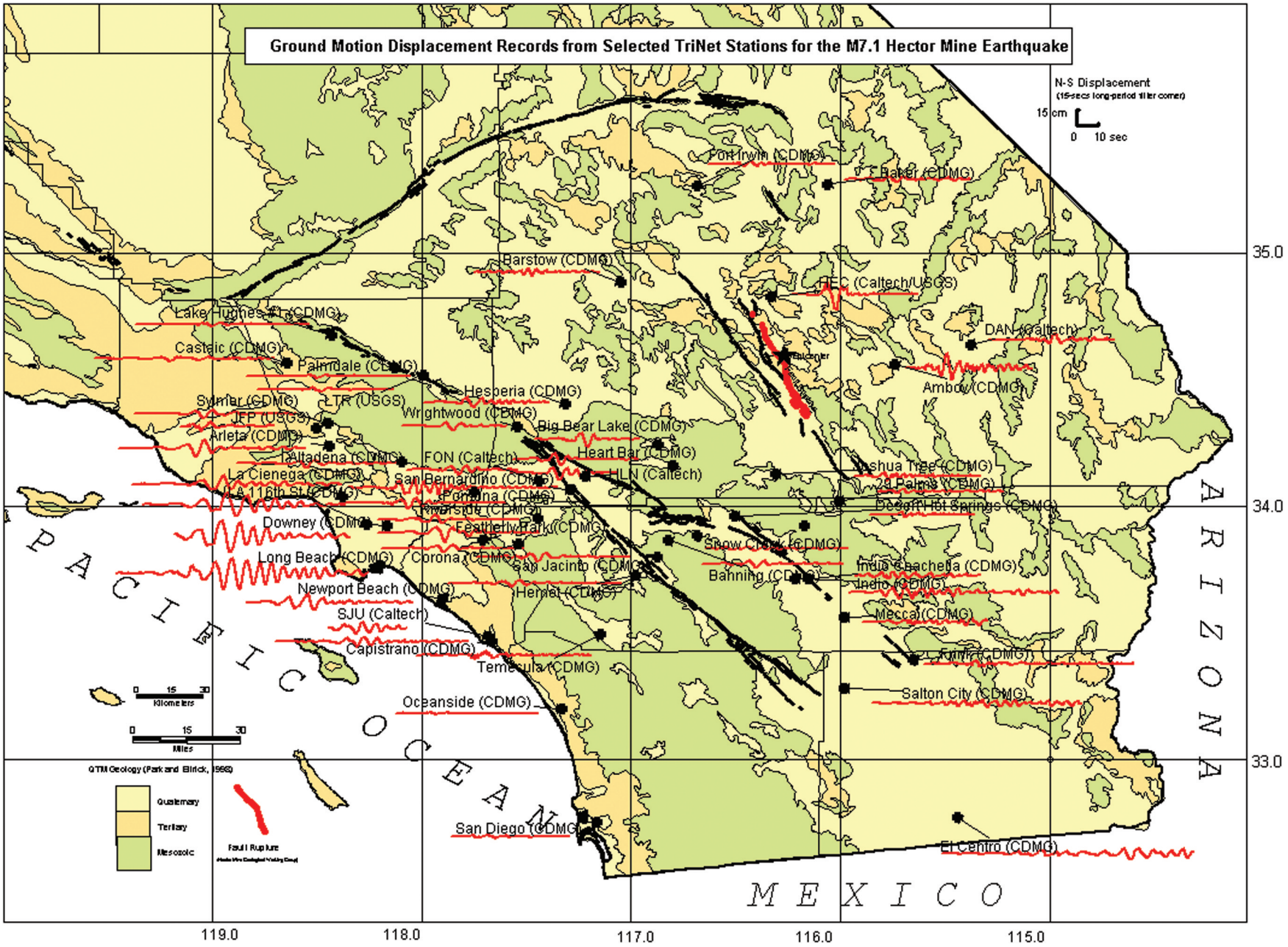

Figure 3. Distribution of N–S component ground displacements of selected stations on the map of southern California with Quaternary, Tertiary, and Mesozoic geology (Jennings, 1977; Park and Elrick, 1998). Surface fault rupture produced by the Hector Mine earthquake (shown in red) is from Treiman *et al.* (2002).

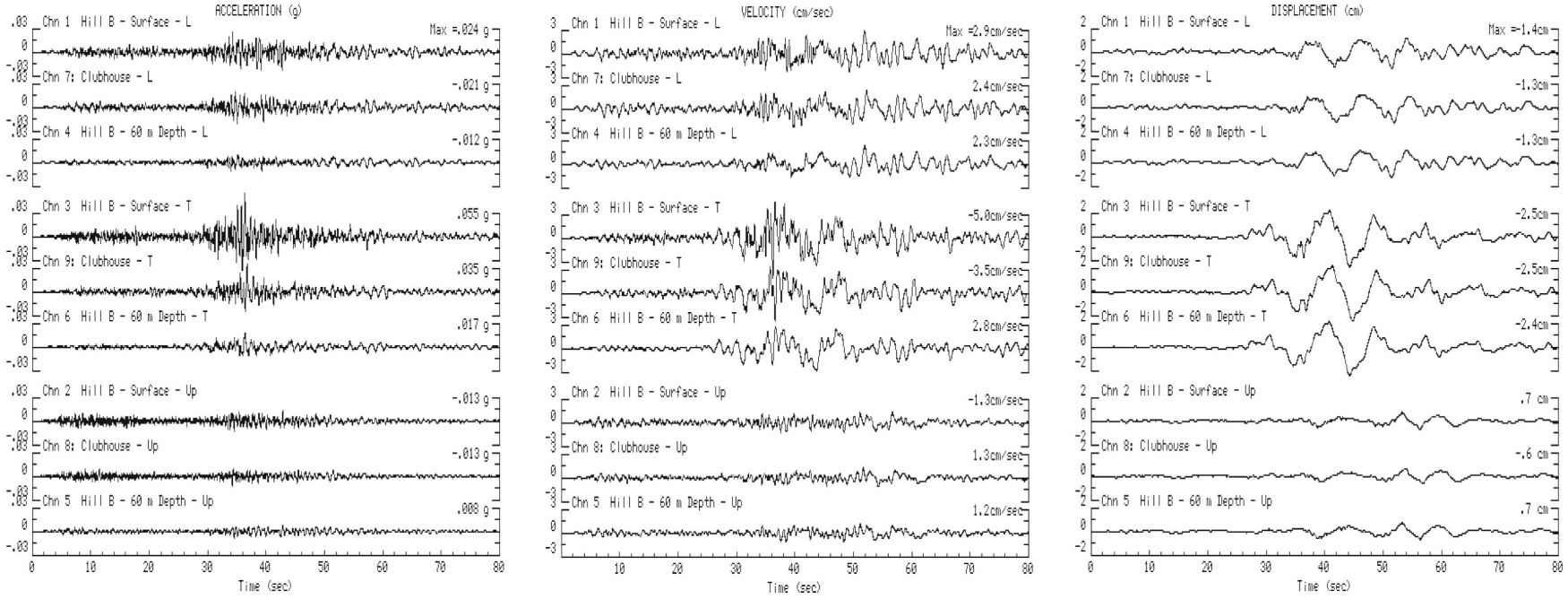

Figure 4. Acceleration, velocity, and displacement recorded at Tarzana during the Hector Mine earthquake at the downhole and the surface site above it, and at the nearby Clubhouse site. Ground motions are shown in directions parallel (L, longitudinal, 75°) and perpendicular (T, tangential, 165°) to the strike of the Tarzana hill.

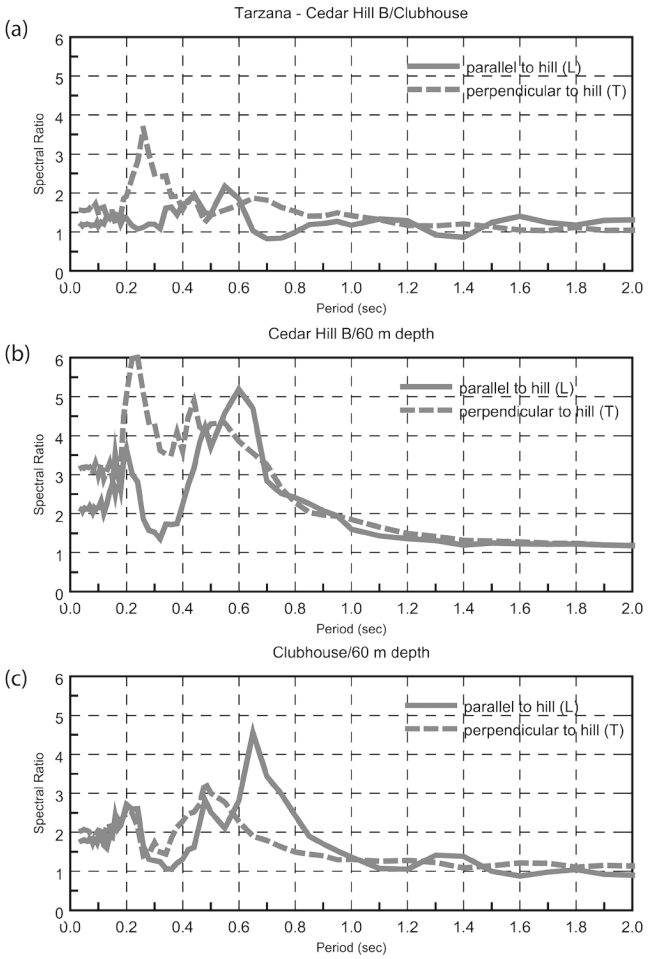

Figure 5. Spectral ratios of the response spectra (5% damped) at Tarzana. Ratios of (a) Cedar Hill B to Clubhouse, (b) Cedar Hill B to 60 m depth, (c) and Clubhouse to 60 m depth for the component parallel to the hill (solid line) and perpendicular to the hill (dashed line).

the surface is more than double along the component perpendicular to the strike of the hill at a period of 0.22 sec (4.5 Hz) (Fig. 5).

Comparison of the response spectra demonstrates clear directional site response resonance at Tarzana hill, with an amplification of more than 3.5 between the foothill station and the top of the hill at a period of 0.3 sec along the component perpendicular to the hill (Fig. 5). This result is similar to previously obtained results from aftershocks of the Northridge earthquake (Vidale *et al.*, 1991; Hartzell *et al.*, 1996; Spudich *et al.*, 1996; Darragh *et al.*, 1998). The three-dimensional topographic effect (Bouchon and Barker, 1996; Catchings and Lee, 1996; Spudich *et al.*, 1996) only partially explains the site amplification on the top of the hill.

Ground Motion Attenuation

Plots of the Hector Mine peak horizontal ground acceleration (PGA), velocity (PGV), and displacement (PGD) recorded by the ground-response stations listed in Table 1 are shown in Figure 6. The PGA, PGV, and PGD demonstrate the differences in amplitude attenuation of different parts of the seismic spectra in the epicentral distance range of 30 to 280 km.

Peak ground acceleration (Fig. 6a) represents the relatively high-frequency part of seismic radiation. It is associated with wave periods of up to 1 sec (frequencies higher than 1 Hz). PGA decreases with increasing epicentral distance to about 150 km, but stays relatively constant at greater distances.

Peak ground velocity (Fig. 6b), representing the mid-range frequencies of 0.1 to 3 Hz (periods of 0.3–10 sec), also demonstrates attenuation, but with much more variability. PGV generally follows the same pattern as PGA, decreasing with epicentral distance and reaching a level of approximately 3 to 5 cm/sec at a distance of about 220 km. It also demonstrates more variability than PGA, especially at epicentral distances of 120 to 220 km.

Peak ground displacement (Fig. 6c), which is mostly associated with the relatively long-period part of the spectrum (generally, 2 sec and longer; frequencies less than 0.5 Hz), shows very high variability and little attenuation with distance, with anomalous amplification at about 160 to 210 km distance from the epicenter. The increased amplification may reflect the shift from motions associated with source-generated *S* waves to the basin-generated or surface waves. PGD reaches a level of approximately 2 to 4 cm at distances greater than 220 km.

Variations in PGA data also are plotted with respect to the closest distance to the fault (in log–log scale) to allow comparison with the Boore–Joyner–Fumal (BJF) (Boore *et al.*, 1993, 1997) relationship between PGA and fault distance. Coefficients for a strike-slip fault and average shear-wave velocity of 520 m/sec in the upper 30 m are used to calculate the empirical prediction BJF97 curve (Fig. 7). This velocity is recommended for use in BJF97 for the National Earthquake Hazards Reduction Program (NEHRP) site class C. The original BJF97 relationship for peak horizontal accelerations is

$$\ln Y = b_1 + b_2(M - 6) + b_5 \ln r + b_v \ln(V_S/V_A), \quad (1)$$

where

$$r = \sqrt{(r_{jb}^2 + h^2)}$$

$b_1 = 0.313$ (for strike-slip earthquakes)
$b_2 = 0.527$, $b_5 = 0.778$
$b_v = 0.371$, $V_A = 1396$ m/sec, $h = 5.57$.

Here M is moment magnitude, r_{jb} is the closest horizontal distance (in km) from the station to the point on the earth's surface that lies directly above the rupture, and V_S is the average shear-wave velocity in the upper 30 m. The equation is limited to distances of 80 km, because of lack of

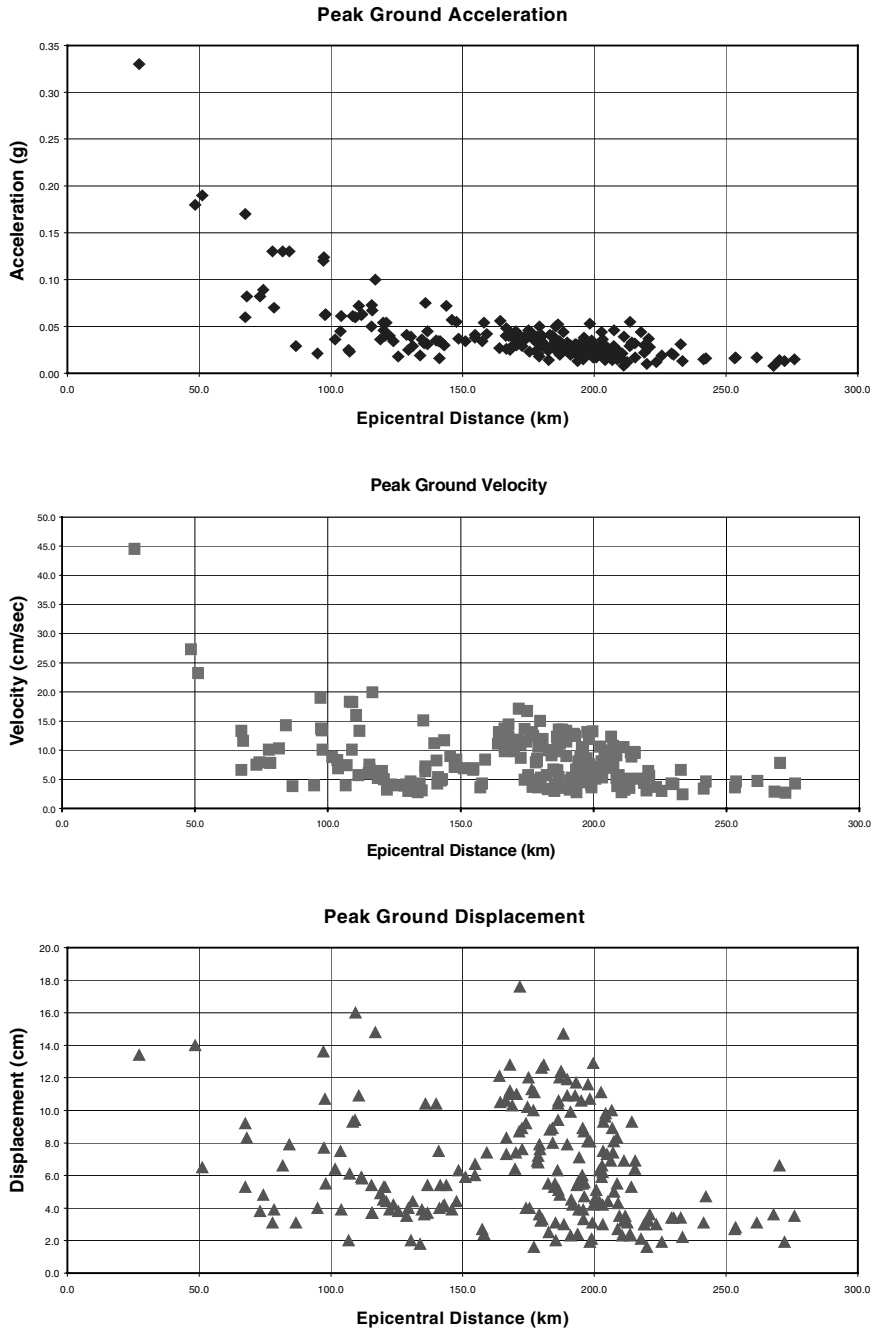

Figure 6. Hector Mine peak ground acceleration (PGA), velocity (PGV), and displacement (PGD) in the epicentral distance range of 30–280 km.

reliable data at greater distances, and to magnitudes $5.5 < M < 7.5$. Peak ground accelerations from the Hector Mine earthquake demonstrate reasonable agreement with the BJF97 attenuation curve in the applicable range and possibly may be used to extend the attenuation relationships to greater distances.

Variations in acceleration, velocity, and displacement dependent upon the azimuth from the epicenter are demonstrated in the record section in Figure 8. Three record sections for the N–S component of ground motion were constructed at azimuths of approximately 255°, 235°, and 215° from the epicenter. To make comparison of the records more convenient, they were shifted so that the maximum phase in displacement of the *S*-wave arrivals are aligned. Accelerations in Figure 8 may be characterized as relatively long wavetrains with varying periods and amplitudes. Velocities also can be characterized by large variations in amplitudes and periods of motions.

Displacements in the 255° azimuth in Figure 8a are similar in amplitude over a large range of epicentral dis-

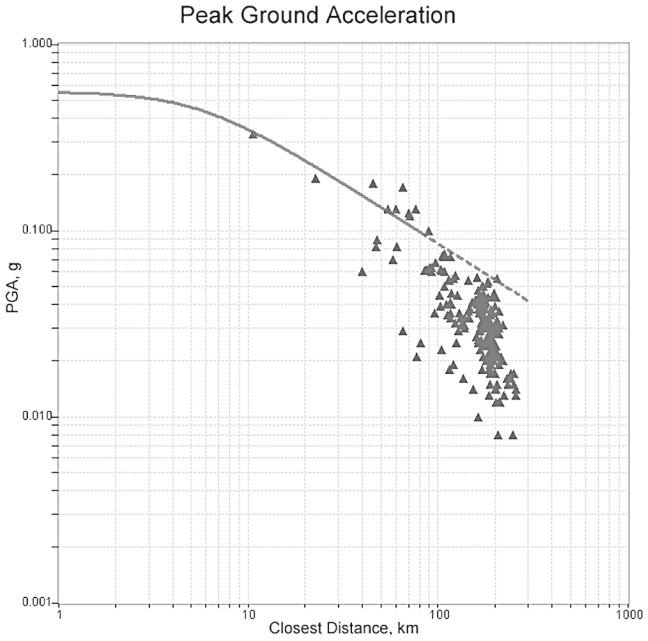

Figure 7. Peak horizontal ground acceleration values plotted against the closest distance to the fault, and the Boore–Joyner–Fumal (Boore *et al.*, 1997) attenuation relationship. For comparison, extrapolation of the BJF97 relationship is shown with dashed line for distances beyond the original distance limitation presented by the authors.

tances, from 100 to 200 km. Displacement records in the azimuth of 215° (Fig. 8c) also demonstrate similarity in shape, but the amplitudes generally decrease with increasing epicentral distance. Displacements at alluvium sites on an azimuth crossing the Los Angeles basin (235°) have the biggest variations in wave shape and duration of oscillation (Fig. 8b). Amplitudes of the motion decrease significantly in the intermediate part of the profile at epicentral distances of 130 to 140 km (e.g., Riverside, Corona) and increase again at distances of 180 to 190 km (e.g., Newport Beach, Huntington Beach).

Large variations in ground motions may be due to the wave-propagation path and near-surface site geology (Tarzana and Temecula) or to the thickness and structure of the sedimentary basin near the station (e.g., San Bernardino, Los Angeles, and Long Beach). For example, ground motion at Temecula (Fig. 8c) has a relatively strong component with a period of 1.4 sec (0.7 Hz), which may be due to the relatively soft surface layer.

Comparison with Landers Earthquake

In contrast to the 1994 Northridge earthquake (M_w 6.7), the Hector Mine event (M_w 7.1) occurred in a desert area relatively far from Los Angeles. From the point of view of its magnitude and location relative to the main urban areas, this earthquake was more similar to the 1992 Landers earthquake (M_w 7.3).

The Landers earthquake was recorded by many strong-motion stations (e.g., Shakal *et al.*, 1992; Cramer and Darragh, 1994), but many of them were film strong-motion accelerograph (SMA) instruments. Relatively few of the Hector Mine earthquake records were recorded by the film instruments, with most of the data being recorded by modern, high-quality digital accelerographs.

A comparison was made of strong ground motions recorded at six stations in the Los Angeles area during the Hector Mine earthquake (epicentral distances of about 190 km) and the Landers earthquake of 1992 (epicentral distances of about 165 km).

For comparison with the Landers earthquake, records at the following stations are studied: Los Angeles–City Terrace, Los Angeles–University Hospital Grounds, Los Angeles–116th street School, Los Angeles–Pico and Sentous, Los Angeles–Temple and Hope, and Los Angeles–Obregon Park. The records of the Landers earthquake used for comparison are reprocessed using the same frequency band 0.067 to 46 Hz (0.022–15 sec) as all the records from the Hector Mine earthquake. The peak horizontal ground accelerations recorded at these six stations are listed in Table 3, and Figure 9 is a comparison of the ground motions at two of the six stations. On average, peak ground accelerations during the Landers earthquake were 1.6 times larger than those of the Hector Mine event.

The response spectra from the 1992 Landers earthquake are higher than for the Hector Mine event, except at periods of 6 to 8 sec, where they are about the same value (Fig. 10). As we have suggested, these periods are most likely associated with the motion in the source of the Hector Mine earthquake. In the 1.5- to 3.0-sec period range, the Landers response spectra are two to three times higher than those of the Hector Mine earthquake. The amplification factor in PGA that one can expect from the difference in magnitude and distance for these two earthquakes using the BJF97 empirical prediction of ground motion gives a factor of 1.24 (Landers PGA/Hector PGA ratio, Table 3). Since the actual peak ground accelerations in the Los Angeles area recorded during the Landers earthquake were 1.6 times larger than the motions during the Hector Mine earthquake, not only differences in location and magnitude are responsible for this effect. Differences in rupturing and directivity of the source processes might also contribute to this amplification effect.

The Landers records are characterized not only by higher amplitudes, but also by longer durations of motion. The longer duration may be explained by the longer rupture length of the earthquake source. Comparison of the surface ruptures associated with the 1992 Landers and the 1999 Hector Mine earthquakes shows that the overall length of the first event was approximately 1.8 time larger (Scientists of the USGS *et al.*, 2000). Using source modeling, the Landers fault length was estimated to be 65 km (Wald and Heaton, 1994) and the length of the Hector Mine source was estimated to be approximately 35 km (Dreger and Kaverina, 2000a,b).

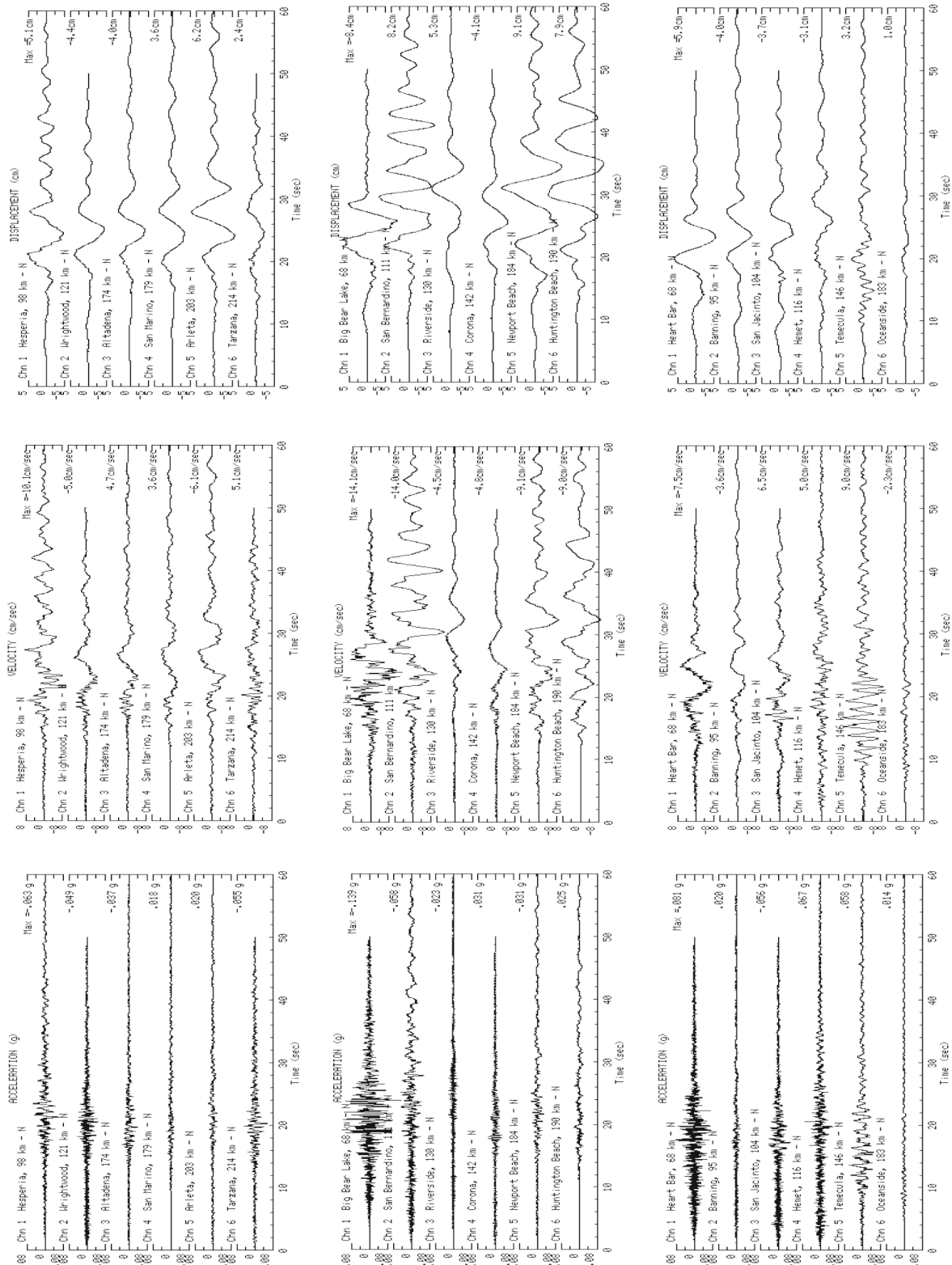

Figure 8. Three record sections of ground motion at azimuths of approximately (a) 255°, (b) 235°, and (c) 215° from the epicenter. The N–S components are shown. The records are shifted in time so that the maximum amplitude of the *S*-wave arrival occurs at the same time.

Table 3
Peak Horizontal Ground Motions in the Los Angeles Area during the Landers and Hector Mine Earthquakes

Station ID	Station Name	Landers		Hector Mine		Landers/ Hector PGA Ratio
		Epi Dist (km)	PGA (*g*)	Epi Dist (km)	PGA (*g*)	
24612	Los Angeles–Pico & Sentous	169.4	0.034	193.9	0.019	1.79
24611	Los Angeles–Temple & Hope	167.6	0.031	191.2	0.027	1.15
24605	Los Angeles–7-story Univ. Hospital Grnds	163.2	0.043	186.9	0.026	1.65
24592	Los Angeles–City Terrace	160.8	0.058	184.8	0.038	1.53
24400	Los Angeles–Obregon Park	161.6	0.065	186.0	0.033	1.97
14403	Los Angeles–116th St. School	171.0	0.042	197.4	0.028	1.50
	Average	165.6	0.0455	190.0	0.0285	1.60
	BJF97	165.6	0.0506	190.0	0.0409	1.24

Summary and Conclusions

A large set of high-quality, mostly digital strong-motion records from more than 300 stations was collected from the Hector Mine earthquake, which occurred in the Mojave Desert. The closest station to the epicenter was approximately 25 km to the north and recorded a peak ground acceleration of 0.33*g*. The two other stations closest to the epicenter were located to the east and south at epicentral distances of about 50 km; these recorded peak ground accelerations of about 0.2*g*.

Two main types of ground displacement waveforms were observed from the Hector Mine earthquake. The first type represents a relatively simple motion with a duration of 15 to 20 sec. This type of motion was observed everywhere, at epicentral distances from 50 km out to 240 km, and may be associated with the source-generated *S* wave. The second type of motion may have high amplitudes (more than 10 cm displacement) at epicentral distances of 160 to 220 km a duration of about 40 seconds long; it has a sinusoidal type waveform with a predominant period of about 5 to 8 sec. The second type of motion appears to be typical for certain locations in the Los Angeles, Long Beach, San Bernardino, and EI Centro areas and most likely is created by Love waves (e.g., by multiple reflections of *S* waves trapped in deep sedimentary basins).

In contrast to other data sets from large earthquakes in California, most of the Hector Mine strong-motion records were obtained at epicentral distances greater than 80 km. In this specific set of data, any directivity effect is less significant than the effect of local and regional geology. This data set may be used to improve existing attenuation relationships, which usually have not had enough reliable strong-motion data for fault distances greater than 100 km. Hector Mine peak ground accelerations (PGA) generally demonstrate reasonable agreement with the attenuation relationship developed by Boore, Joyner, and Fumal (Boore *et al.*, 1997), which was developed for fault distances less than 100 km because adequate data were not available at greater distances.

Peak ground displacements (PGD), with relatively large amplitudes recorded at epicentral distances of 160 to 220 km, do not demonstrate a normal attenuation pattern. Strong-motion data recorded in Los Angeles, Long Beach, and some other areas demonstrate significant, apparently basin-amplified wave amplitudes, especially at periods of 5 to 8 sec. This may reflect control by the sedimentary basin of the high-amplitude, long-period waves seen in the time domain.

Records from the Tarzana hill again demonstrated unusually high amplitudes of acceleration compared to the record at the foot of the hill. This site amplification effect has a clear directional character, with higher amplification along the component perpendicular to the strike of the hill. The source of the site amplification that produces large motions at Tarzana is still under investigation.

Comparisons of ground motions recorded from the M_w 7.1 Hector Mine and the M_w 7.3 Landers earthquakes indicate that the Landers records not only had higher amplitudes, but also had longer durations of ground motion. For the Los Angeles area, the Landers response spectra were on average two to three times higher than those of the Hector Mine event, except at periods of 6 to 7 sec, where they were about the same value.

Processed data from ground-response stations and a number of buildings and bridges were made available quickly after the earthquake at *ftp://ftp.consrv.ca.gov/pub/dmg/csmip/Hector_Mine/* (now *HectorMine 99*). Additional records of the USGS, CDMG, and other networks continue to be collected and verified and will be put on the TriNet/CISN Web site (*http://www.cisn.org*).

Acknowledgments

The TriNet networks extend their appreciation to the individuals and organizations that have permitted and cooperated in the installation of seismic strong-motion equipment on their property. The records presented in this paper were made possible through the efforts of technicians who installed and maintained these stations. The authors thank Bill Bryant for providing a digital file of the surface rupture associated with the Hector Mine earthquake. The authors also thank Tianquing Cao for assistance in digitizing and data processing, and Jim Agnew and Hamid Haddadi for

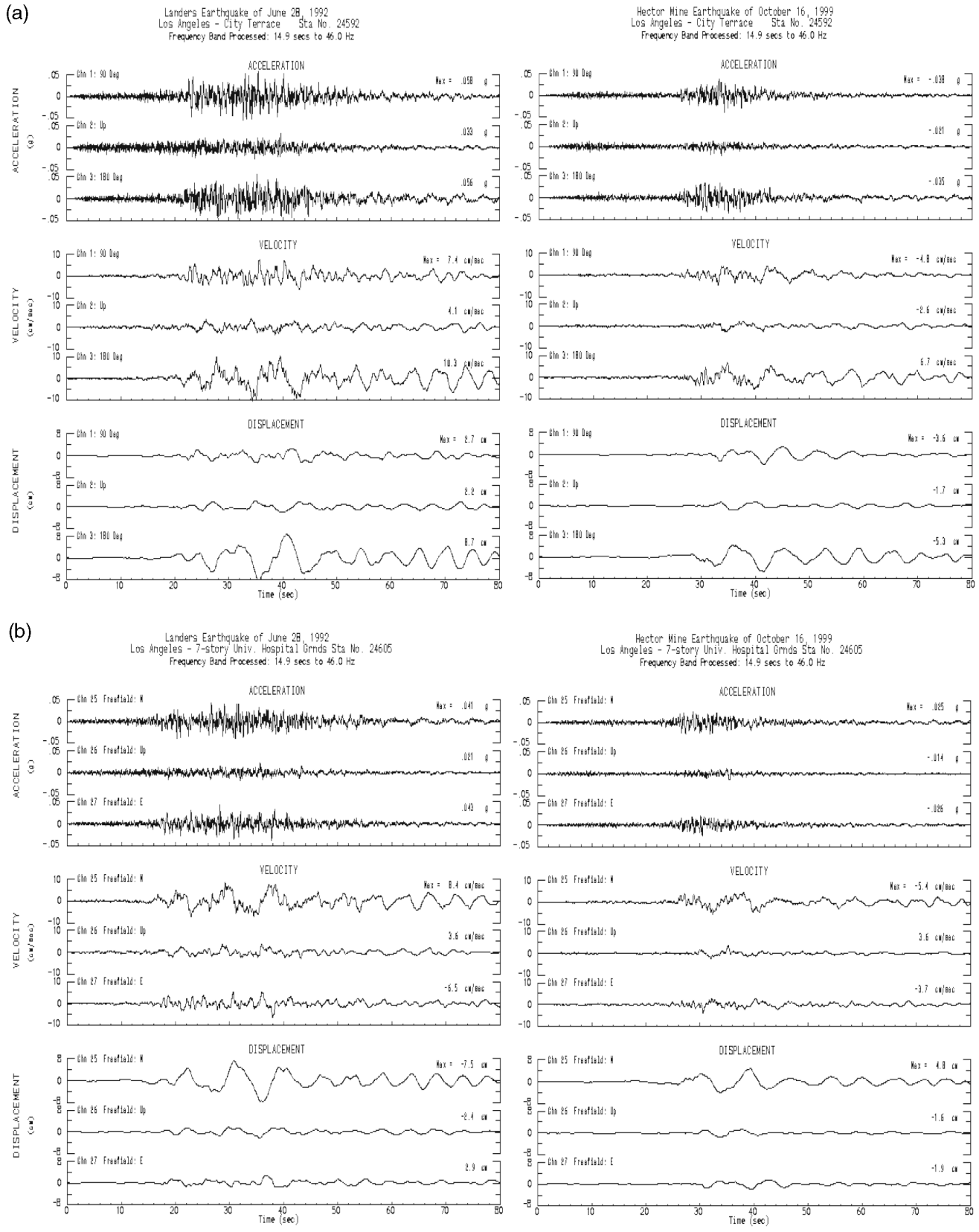

Figure 9. Strong ground motions recorded at two stations in the Los Angeles area during the Hector Mine earthquake and the Landers earthquake of 1992: (a) Los Angeles–City Terrace; (b) Los Angeles–University Hospital Grounds.

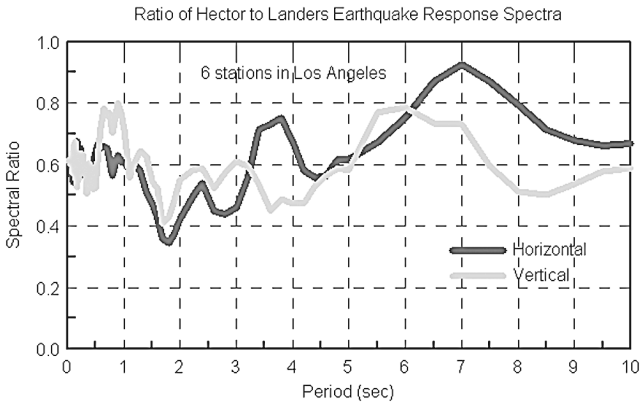

Figure 10. Ratios of the average response spectra (5% damped) for the six stations in the Los Angeles area comparing the Hector Mine earthquake to the Landers earthquake of 1992.

reviewing the manuscript. The manuscript benefited from comments of Michael Rymer and two anonymous reviewers.

References

Boore, D. M., W. B. Joyner, and T. E. Fumal (1993). Estimation of response spectra and peak accelerations from western North American earthquakes: an interim report, *U.S. Geol. Surv. Open-File Rept. 93–509*.

Boore, D. M., W. B. Joyner, and T. E. Fumal (1997). Equations for estimating horizontal response spectra and peak acceleration from western North American earthquakes: a summary of recent work, *Seism. Res. Lett.* **68,** no. 1, 128–153.

Bouchon, M., and J. S. Barker (1996). Seismic response of a hill: the example of Tarzana, California, *Bull. Seism. Soc. Am.* **86,** no. 1A, 66–72.

Catchings, R. D., and W. H. K. Lee (1996). Shallow velocity structure and Poisson's ratio at Tarzana, California, strong-motion accelerometer site, *Bull. Seism. Soc. Am.* **86,** 1704–1713.

Cramer, C. H., and R. B. Darragh (1994). Peak accelerations from the 1992 Landers and Big Bear, California, earthquakes, *Bull. Seism. Soc. Am.* **84,** no. 3, 589–595.

Darragh, R., V. Graizer, and A. Shakal (1997). Site characterization and site response effects at CSMIP stations: Tarzana and La Cienega near the Santa Monica freeway (1–10). California Strong Motion Instrumentation Program, OSMS 96-07, Sacramento, California, 15 January 1997, 262 pp.

Darragh, R., V. Graizer, and A. Shakal (1998). Tarzana, California: site response and characterization, in *Proceedings of the NEHRP Conference and Workshop on Research on the Northridge, California Earthquake of January 17, 1994*, Vol. II, 323–330.

Dreger, D., and A. Kaverina (2000a). Seismic remote sensing for the earthquake source process and near-source strong shaking: a case study of the October 16, 1999 Hector Mine earthquake, *Geophys. Res. Lett.* **27,** no. 13, 1941–1944.

Dreger, D., and A. Kaverina (2000b). Source process of the October 16, 1999 Hector Mine earthquake, in *Berkeley Seismological Laboratory Annual Report*, July 1999–June 2000, 100–101.

Graizer V. M., T. Cao, A. F. Shakal, and P. Hipley (2000a). Data from downhole arrays instrumented by the California Strong Motion Instrumentation Program in studies of site amplification effects, in *Proceedings [CD-ROM] of the Sixth International Conference on Seismic Zonation (61CSZ)*, Earthquake Engineering Research Institute, Palm Springs, California, 12–15 November 2000.

Graizer V. M., A. F. Shakai, and P. Hipley (2000b). Recent data recorded from downhole geotechnical arrays, in *Proceedings of SMIP2000 Seminar on Utilization of Strong-Motion Data*, Sacramento, California, 14 September 2000, 23–38.

Hartzell, S., A. Leeds, A. Frankel, and J. Michael (1996). Site response for urban Los Angeles using aftershocks of the Northridge earthquake, *Bull. Seism. Soc. Am.* **86,** no. 1B, S168–S192.

Hauksson, E., L. M. Jones, and K. Hutton (2002). The 1999 M_w 7.1 Hector Mine, California, earthquake sequence: complex conjugate strike-slip faulting, *Bull. Seism. Soc. Am.* **92,** 1154–1170 (this issue).

Jennings, C. W. (1977). Geologic map of California. Scale 1:750,000. California Division of Mines and Geology, Sacramento, California 95814.

Jennings, C. W. (Compiler) (1994). Fault activity map of California and adjacent areas, California Department of Conservation, Division of Mines and Geology, Geologic Data Series No. 6, scale 1:750,000.

Mori, J., H. Kanamori, J. Davis, E. Hauksson, R. Clayton, T. Heaton, L. Jones, and A. Shakal (1999). Major improvements in progress for southern California earthquake monitoring, *EOS* **79,** 217–221.

Park, S., and S. Elrick (1998) Prediction of shear-wave velocities in southern California using surface geology, *Bull. Seism. Soc. Am.* **88,** no. 3, 677–685.

Scientists of the U.S. Geological Survey, Southern California Earthquake Center, and California Division of Mines and Geology (2000). Preliminary report on the 16 October 1999 *M* 7.1 Hector Mine, California, earthquake, *Seism. Res. Lett.* **71,** no. 1, 11–23.

Shakal, A., M. Huang, and T. Cao (1988). The Whittier Narrows, California earthquake of October 1, 1987: CSMIP strong motion data, *Earthquake Spectra* **4,** 75–100.

Shakal, A., M. Huang, T. Cao, R. Sherburne, R. Sydnor, P. Fung, P. Malhotra, C. Cramer, F. Su, R. Darragh, and J. Warnpole (1992). CSMIP strong-motion records from the Landers, California earthquake of 28 June 1992. California Strong Motion Instrumentation Program, OSMS 92-09, Sacramento, California, August 5, 1992, 330 pp.

Shakal, A. F., M. J. Huang and R. B. Darragh (1996). Interpretation of significant ground-response and structure strong motions recorded during the 1994 Northridge earthquake, *Bull. Seism. Soc. Am.* **86,** no. 1B, S231–S246.

Shakal, A., M. Huang, R. Darragh, T. Cao, R. Sherburne, P. Malhotra, C. Cramer, R. Sydnor, V. Graizer, G. Maldonado, C. Petersen and J. Wampole (1994). CSMIP strong-motion records from the Northridge, California earthquake of 17 January 1994, California Strong Motion Instrumentation Program, OSMS 94-07, Sacramento, California, 18 February 1994, 308 pp.

Spudich, P., M. Hellweg, and W. H. K. Lee (1996). Directional topographic site response at Tarzana observed in aftershocks of the 1994 Northridge, California, earthquake: implications for mainshock motions, *Bull. Seism. Soc. Am.* **86,** no. 1B, S193–S208.

Treiman, J. A., K. J. Kendrick, W. A. Bryant, T. K. Rockwell, and S. F. McGill (2002). Primary surface rupture associated with the M_w 7.1 16 October 1999 Hector Mine earthquake, San Bernardino County, California, *Bull. Seism. Soc. Am.* **92,** 1171–1191 (this issue).

Vidale, J. E., O. Bonamassa, and H. Houston (1991). Directional site resonances observed from the 1 October 1987 Whittier Narrows, California, earthquake and the 4 October aftershock, *Earthquake Spectra* **7,** 107–125.

Wald, D. J., and T. H. Heaton (1994). Spatial and temporal distribution of slip for the 1992 Landers, California, earthquake, *Bull. Seism. Soc. Am.* **84,** no. 3, 668–691.

California Division of Mines and Geology
Strong Motion Instrumentation Program
801 K Street, MS 13–35
Sacramento, California 95814
vgraizer@consrv.ca.gov
(V.G., A.S.)

California Division of Mines and Geology and
California Institute of Technology
Pasadena, California 91125
(C.S.)

California Institute of Technology
Pasadena, California 91125
(E.H., J.P.)

U.S. Geological Survey
Pasadena, California 91106
(L.J.)

Manuscript received 23 January 2001.